PHYSICAL REVIEW B **81**, 195417 (2010)

Study of defects in Pd thin films on Au(100) using molecular dynamics

Z. S. Pereira and E. Z. da Silva
Institute of Physics "Gleb Wataghin," University of Campinas (UNICAMP), 13083-970 Campinas, SP, Brazil
(Received 6 August 2009; revised manuscript received 6 April 2010; published 10 May 2010)

We used molecular dynamics with embedded-atom method to model the growth of a Pd thin film deposited on Au(100) for a system with approximately 100 000 atoms. We showed that the Pd film grew under stress on the Au substrate with face-centered-cubic structure. After the deposition of 9 monolayers, the stress stored in the Pd film relaxed with the formation of defects, stacking faults in the structure of Pd forming a pattern of deformation in the film. We analyzed the structures obtained in the simulation using the centrosymmetry parameter and angular distribution functions proposed by Ackland and Jones. Analysis of monolayer spacing, coordination number, and normal compressive strain for small deformation are presented. To quantitatively access the defect formation we also measured the stress tensor evolution during growth, which clearly showed the change in structure. All these results were in agreement with the structure analysis giving a nice understanding of the formation of these defected structures.

DOI: 10.1103/PhysRevB.81.195417 PACS number(s): 68.55.−a, 68.65.Ac, 68.35.Gy, 68.35.Ct

I. INTRODUCTION

The development of new experimental techniques in the last two decades of the last century started the new field of nanoscience, allowing detailed study of atomic structures, renewed the interest in the effect of defects during the growth process of thin films on surfaces and in nanostructures. There is also hope that some of the new developments can result in technological applications for the new generations of devices. One interesting example is face-centered-cubic (fcc) metals that upon growth on fcc substrates do so in different phases. Using Au(100) and Ag(100) as substrates it is possible to grow body-centered-cubic (bcc) Cu films using those substrates as templates. The 12% mismatch between the host lattice and the deposited film produces the desired effect that have been reported experimentally[1,2] and discussed theoretically using computer simulations.[3] When other metals are deposited on Au(100) other kinds of effects can be produced depending, for example, on the host/film mismatch and also on temperature.

The present work investigates the growth process of Pd on Au(100). When Pd is deposited on Au(100) a Pd fcc phase is formed under stress conditions. As the process continues with more layers deposited, defects as stacking faults are formed. In this study, the growth process and the effect of defects is performed using classical molecular dynamics (MD). It is worth stressing that Pd has been intensively studied because of its catalytic properties,[4] and although Pd is a paramagnetic material in its stable fcc phase, many experimental studies have observed strong evidences of ferromagnetic-moment formation in nanoparticles of Pd.[5–9] Such magnetic behavior is attributed to expanded volumes, changes in the crystal symmetry or defects in the fcc lattice, e.g., stacking faults and twin boundaries. This was also verified in theoretical works with small Pd clusters.[10–12] Defects such as stacking faults break the cubic symmetry of (111) stacking sequence forming hexagonal-closed-packed (hcp) structures. They are a common type of defect because the formation of stacking faults needs small amounts of energy, and therefore it is difficult to avoid their formation in the thin-film growth process.

In the growth of the thin films, surface stress due to the lattice mismatch between deposited film and substrate may also give rise to periodic deformation patterns after some monolayers are deposited. Stripes or even moire patterns can occur to relax stress. Examples include stripes in Au on W(110),[13] Cu on Au(100), Cu on Ag(100),[1–3] hexagonal moire structure in Pb on Ag(100) or Ag(111),[14] square-shaped moire pattern in Cu on Pt(100) (Ref. 15), and as reported recently, stripes in Pd on W(110).[16]

All these facts and findings motivated us to study thin films of Pd grown on Au(100). A way to produce stress in a stable Pd bulk is to grow it on substrates with square symmetry and lattice constant larger than the stable fcc Pd lattice parameter. For the first few monolayers (ML) deposited, the Au substrate acts as a template for the Pd atoms to form Pd fcc phase under tensile stress. Therefore, Pd atoms grew pseudomorphic to the Au substrate with biaxial expansion of their crystallographic parameters a and b and compression along c. In the present simulation, Pd films grew layer by layer in agreement with findings of Liu and Barder[17] that reported, based on low-energy electron diffraction experiments, that there is a layer-by-layer growth for Pd on Au(100) at 300 K. The Pd film grew with fcc structure under stress with parameters a and b approximately expanded by 4.8%. After a critical thickness the structure of Pd film relaxed and stacking-faults-type defects emerged at (111) planes of the crystal. The present work simulated the crystal growth of Pd on Au(100). The results provided a detailed description of the formation of defects that were analyzed using two complementary techniques to study the underlying structures formed. In order to make these findings quantitative we also studied the evolution of the calculated stress tensor during the growth process, which showed very good agreement with the structural analysis.

This paper is organized as follows: in Sec. II we discuss the potential and computational procedures. Section III presents the results/discussion and it is divided in three parts. In the first part (Sec. III A) the structures of Pd thin film were determined as fcc, bcc, or hcp, the monolayers spacing and coordination number were analyzed. In the second part (Sec III B) the structure was also analyzed, but now, looking for

departures from the fcc symmetry due to extended defects. In the third part (Sec. III C) a quantitative calculation of the evolution stress tensor during the growth process is discussed. Finally Sec. IV presents conclusions.

II. POTENTIAL AND COMPUTATIONAL PROCEDURE

In this study, we used molecular dynamics with many-body effective potentials based on the embedded-atom method (EAM),[18–20] using the LAMMPS code[21] to model the deposition of Pd on Au(100). EAM potentials are fitted to reproduce some properties of the system studied. This makes EAM a good model for problems of expansion and compression of bulk metal where the fit of elastic constants is important to reproduce accurately mechanical properties of many metals. Furthermore, this method showed excellent transferability and has been largely used in computer simulations. Calculations using *ab initio* methods to study the electronic states become prohibitive when systems are so large such as the one studied in this work (up to 100 000 atoms). However, using MD with the EAM potential we can verify the formation of a moire pattern of defects in the Pd film caused by formation of defects in the growth process of the type of stacking faults.

We considered three different EAM potentials, the Foiles potential[20] that is fitted to exactly reproduce the equilibrium lattice constant, the sublimation energy, elastic constants and vacancy-formation energy for pure metals, and the heats of solution of the binary alloys. The Zhou potential[19] which has an analytic form for the potential fitted to experimental values and the Bin potential[18] which is a modification of the Zhou potential also parameterized to include fitting to density-functional-theory calculations of bulk properties of the Pd-Au alloy and of metal clusters.

The present work discusses the growth of Pd thin film on Au(100) and the important processes associated with it, such as the formation of stacking faults to release the accumulated stress, therefore it is important to comment on the stacking-fault energies (γ_{sf}).[22] In fact, more important than stacking-fault energies is a discussion of the generalized planar-fault (GPF) energy curve for stacking faults which is more appropriate since it gives a better understanding of the formation of these defects than just the stacking-fault energy γ_{sf}. In Fig. 1 we show the GPF energy curve calculated with three effective potentials used in the present work.[18–20] It shows the energy cost for a slip over the (111) plane along the $[11\bar{2}]$. The energy barrier γ_{us} is the lowest value to be overcome for the occurrence of a stacking fault with energy γ_{sf}. The calculated values were $\gamma_{sf}=85$ mJ/m^2 for the Bin potential,[18] $\gamma_{sf}=55$ mJ/m^2 for the Zhou potential,[19] and $\gamma_{sf}=51$ mJ/m^2 for the Foiles potential,[20] while the experimental value is 130 mJ/m^2.[23] The unstable stacking-fault energy gave values $\gamma_{us}=218$ mJ/m^2, $\gamma_{us}=187$ mJ/m^2, and $\gamma_{us}=162$ mJ/m^2 for Bin, Zhou, and Foiles potentials, respectively. More important than that it gives the ratio $\gamma_{sf}/\gamma_{us}=0.39$ (Bin potential) showing a good stability of the stacking faults. Furthermore, a complete dislocation for the Bin potential in the [110] direction was calculated as 646 mJ/m^2 (not shown in Fig. 1). Therefore a complete dislocation in the [110] direction, even if split into partials, would have a considerably higher energy barrier and for that reason they are not observed. This shows that the use of these potentials can provide a reasonable modeling for the phenomena. Since the Bin potential gave the best stacking-fault energy, we present in the following sections results only for this potential. Nevertheless the calculations performed using these three potentials obtained qualitatively the same results.

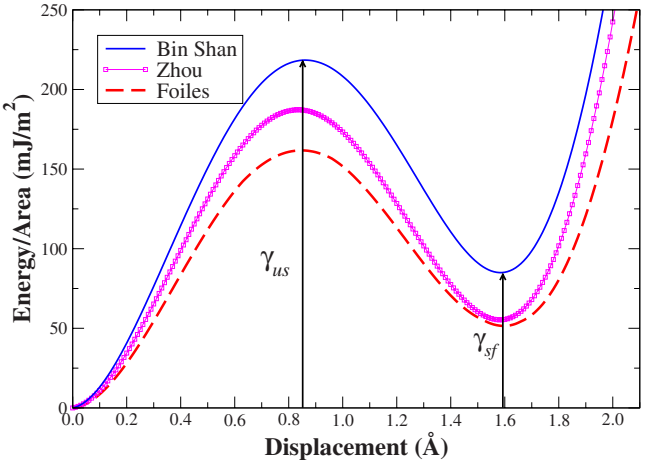

FIG. 1. (Color online) The GPF energy curve for stacking faults for slip over the (111) plane along the $[11\bar{2}]$. γ_{sf} is the stacking-fault energy and γ_{us} is the unstable stacking-fault energy.

We deposited Pd on Au(100) with a similar method reported in Ref. 3. Initially, the Au substrate of dimensions $13.4\times13.4\times6.1$ nm^3 was relaxed by 300 ps. The velocity Verlet algorithm was used to integrate the equations of motion in the canonical ensemble. The substrate was formed by 31 layers and kept at a temperature of 300 K using a Nose-Hoover thermostat.[24] After relaxation of the substrate, we randomly deposited Pd atoms on Au(100), such that, on average, one monolayer was deposited every 200 ps and further relaxed for 200 ps for the calculation of the stress thickness product. We used periodic boundary conditions for the lateral faces while the growth direction was left free from constraints except for the substrate bottom, where three layers kept frozen. The simulation time of the deposition process was 6.3 ns using a time step of 1 fs.

All results presented in the following sections were obtained at the temperature of 300 K. In order to show that the obtained structures are robust in a wide range of temperatures, after deposition of the entire film, the temperature was gradually ramped from 300 to 600 K in 300 ps. It was then maintained at 600 K for 200 ps and finally linearly reduced to 100 K in 500 ps. The simulation time of this annealing was 1.0 ns using a time step of 1 fs. The observed structures after this procedure were essentially the same as the ones studied at 300 K.

III. RESULTS AND DISCUSSION

The crystalline structures obtained from molecular-dynamics simulations, were analyzed using angular-

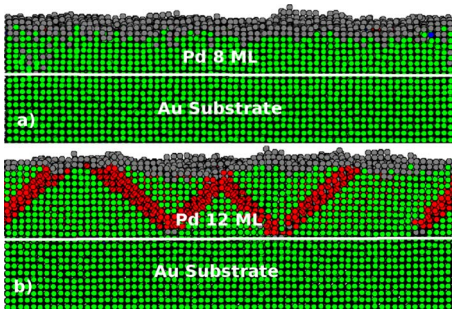

FIG. 2. (Color online) Green (gray) indicates atoms in a local environment with fcc structure, blue (black) indicates bcc structure, red (dark gray) means hcp structure, and gray (light gray) are atoms that Ackland-Jones method did not identifiy their local structure. Only part of the substrate is shown in the [100] direction.

distribution functions as reported recently by Ackland and Jones.[25] Centrosymmetry parameter was used to measure possible inversions of symmetry in the fcc structure (discussed in Sec. III B). The Ackland-Jones method (AJM) is based on the analysis of angular distribution function of perfect crystalline lattices as well as lattices with small distortions generated in simulations. With an heuristic algorithm[25] it is decided which kind of local environment (structure) each atom belongs to. Since each structure has a particular angular distribution function, the method enabled us to decide between fcc or hcp structures even at high temperatures.[25] The evolution of the stress tensor is also discussed.

A. Analysis of the structure and strain

The structures developed in the molecular-dynamics simulation of the thin-film growth and the results obtained with AJM are shown in the Fig. 2(a), shows the structure after 8 ML were deposited on Au(100), suggesting that the first monolayers has grown epitaxially with fcc structure. The Ackland-Jones method indicated that Pd grew in the fcc structure as it is found in nature. Although these structures are fcc, we will see in Sec. III C that Pd grew under stress and, therefore, we have an unstable fcc structure for the Pd film. After that, when more layers of Pd were deposited, the whole structure of Pd film relaxed and well-defined planar defects appeared, symmetric about (111) surfaces identified by AJM as hcp structure [see Fig. 2(b)]. A break in the fcc symmetry occurred in the stacking sequence in the (111) direction, changing from a cubic sequence of planes to a hexagonal sequence through a partial dislocation in some (111) planes. Figure 3 shows slices in the (100) direction of Pd film at different depths analyzed by AJM after the growth of 15 layers of Pd. This showed a regular pattern for these defects in the crystal structure.

Furthermore, the measured average spacing among monolayers of Pd for the first deposited monolayers (up to 6 ML) gave a value of 1.8 Å, shorter than the 1.94 Å for stable bulk Pd. The normal compressive strain (Δ) in the [100] direction for small deformations is given by $\Delta=(d_{film}-d_{bulk})/(d_{film})$,[26] where d_{film} and d_{bulk} are the interlayer distances of the film and the bulk Pd, respectively. For the Pd film $\Delta=-8\%$.

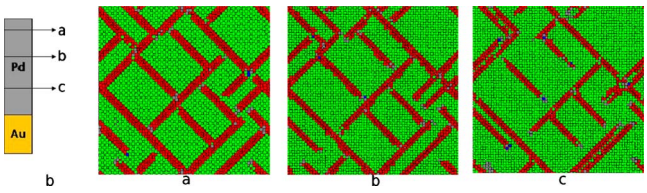

FIG. 3. (Color online) The analysis made with AJM after deposition of 15 ML of Pd on Au(100). Slices of the Pd thin film in the [100] direction were taken: (a) 10 ML, (b) 6 ML, and (c) 3 ML. Green (gray) indicates atoms in a local environment with fcc structure, red (dark gray) means hcp structure, blue indicates bcc structure, and gray (light gray) are atoms that the Ackland-Jones method did not identify their local structure.

The coordination number was calculated for the whole film, we obtained a value 12 for all atoms, except for the surface atoms. This is in agreement with an fcc structure having defects of the type stacking fault where such defects do not change the coordination number. For this calculation we used a cut-off ratio of 3.1 Å for Pd-Pd and 3.25 Å for Au-Au and Pd-Au interface.

B. Analysis of the centrosymmetry parameter

Another method, based on a different principle in comparison with AJM, was used to characterize the structures in the film. The centrosymmetry parameter ($\boldsymbol{c}$) is a method widely used for identifying defects in crystals, such as stacking faults.[27–29] In some cases, defects can have a mathematical role, and then, it is possible, mathematically speaking, to define accurately some defects and to measure the degree of inversion symmetry in each atom based on local environment. The centrosymmetry parameter implements this strategy. To measure the centrosymmetry parameter $\boldsymbol{c}$, we used the expressions[28]

$$D_j = |\mathbf{d}_1 + \mathbf{d}_j|^2, \tag{1}$$

$$c_i = \frac{\sum_{k=1}^{m_i/2} D_k}{2\sum_{j=1}^{m_i} |\mathbf{d}_j|^2}. \tag{2}$$

Choosing one atom i, $|\mathbf{d}_j|$ is the distance of i to another atom j. $|\mathbf{d}_1|$ is the smallest distance between a j atom to atom i within a set with m_i nearest-neighbor atoms to atom i, where $m_i=\min(M,N_i)$, M is the most populous coordination number of the lattice and N_i is the coordination number of atom i. In Eq. (1), d_j is chosen to minimize the vector function D_j. The obtained D is summed in Eq. (2). This pair of atoms used in this procedure are removed from the set and the process to obtain a new D_j is repeated $m_i/2$ times for each i atom to obtain the centrosymmetry parameter $\boldsymbol{c}$.

In a perfect stacking fault (intrinsic) the centrosymmetry parameter is equal to 0.0416.[28] For a perfect fcc crystal the

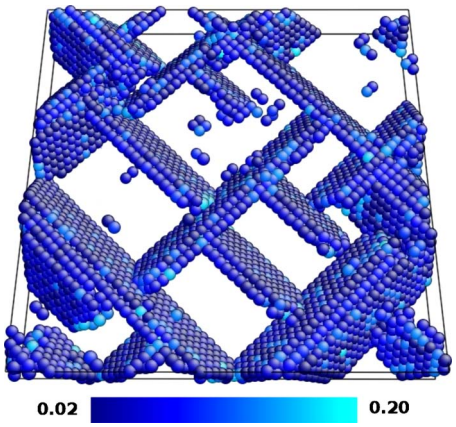

FIG. 4. (Color online) Results obtained for calculation of the centrosymmetry parameter c. Almost all atoms presented c in a range $0.04 < c < 0.08$, except atoms in the surfaces (top and bottom layers).

centrosymmetry parameter is zero and even at high temperature c should be less than 0.01,[28] therefore, it is possible to discriminate between stacking faults and thermal noise. The result obtained with the centrosymmetry parameter is shown in the Fig. 4. The calculation was made for the whole system [Pd/Au(100)]. Only atoms with $0.02 < c < 0.20$ are shown. Note that only some (111) surfaces are shown. Most of the atoms displayed presented $0.04 < c < 0.08$ in accordance with the expected value for stacking faults. All other atoms, except, atoms of the top Pd layer or bottom Au layer, presented $c < 0.02$ in accordance with the fcc structure. As we can see from Figs. 2–4, although we have different methods (methods with different fundamental principles) to analyze the structures, both, AJM and centrosymmetry parameter were in agreement with both the location and the type of defects produced. AJM indicated an hcp structure for the same planes where centrosymmetry parameter indicated values for c in agreement with the formation of stacking faults.

C. Stress evolution

In order to further understand the processes into play during the film growth we also measured the evolution of the stress tensor of the film. While the results presented in the previous section were structural in nature, here we discuss the energetic reasons for such evolution. The evolution of the stress tensor gives quantitative information on the type of growth, it clearly discriminates compressive stress evolution and tensile evolution and therefore is an interesting tool to quantitatively understand the processes that are occurring in the film growth. The present calculation of the stress tensor quantitatively showed a clear change in stored energy with the film-growth evolution, clearly marking the departure from stressed fcc to relaxed fcc structure with staking faults. The virial stress tensor evolution in the Pd film was measured using the Eq. (3) in a similar way as described in Refs. 30–33. The mean virial stress is equivalent to the continuum Cauchy stress.[33] The equation is given by

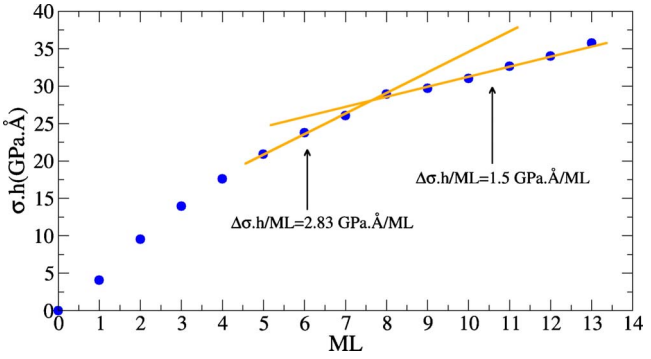

FIG. 5. (Color online) Calculation of the stress-thickness product as function of the number of deposited monolayers.

$$\Pi^{\alpha\beta} = -\frac{1}{\Omega}\left\{\sum_i m_i v_i^\alpha v_i^\beta + \frac{1}{2}\sum_i \sum_{i\neq j} F_{ij}^\alpha r_{ij}^\beta\right\}, \tag{3}$$

where Ω is the volume of the system, m_i is the mass of the i atom, and v_i is its velocity in the direction α, where the indices α and β denote the Cartesian coordinates, and r_{ij}^β is the β component of the vector that separates atoms i and j. As described in Refs. 30 and 31 we calculate the stress-thickness product, $\sigma_{xx} \cdot h$, that can be measured experimentally, and is given by

$$\sigma_{xx} \cdot h = (F_x - F_x^0)/L_y, \tag{4}$$

where $F_x = (\Pi^{xx}\Omega)/L_x$ is calculated for all atoms of the system, F_x^0 is calculated only for atoms of the Au substrate before deposition, and h is the thickness of the film. After that, we took the average between σ_{xx} and σ_{yy}, to get the stress-thickness product

$$\sigma \cdot h = (\sigma_{xx} \cdot h + \sigma_{yy} \cdot h)/2. \tag{5}$$

Figure 5 shows the calculated stress-thickness product versus the number of deposited monolayers. Each data point represents the calculated stress thickness averaged over 40 000 measurements at 40 ps after 160 ps MD relaxations. The graph shows that the incremental film stress (the slope of the $\sigma \cdot h$ curve) is positive showing a tensile stress being stored into the fcc Pd film. As the growth evolved, at a certain point (after 8 ML) the slope changed to a lower value showing the release of the accumulated stress in the film with the formation of stacking faults. The calculated incremental film stress is approximately linear up to 8 ML and gave a value $(\Delta\sigma \cdot h)/\mathrm{ML} = 2.83$ GPa Å/ML. From the 9 ML up to 13 ML the slope changed to $(\Delta\sigma \cdot h)/\mathrm{ML} = 1.5$ GPa Å/ML, indicating a relaxation in the structure of Pd film in agreement with both AJM that showed formation of hcp structure and centrosymmetry parameter that showed a change in symmetry of the Pd fcc phase in some (111) planes. In the analysis of the stress tensor it is possible see that after 8 deposited ML, the film started the relaxation process. The consequences of which only started to be observed in the analysis of the AJM and the centrosymmetry parameter by the formation of other symmetry structures after 9 ML.

Although there are some experiments of Pd growth on Au(001) they diverge about the number of Pd monolayers that can grow layer by layer. It was related 6, 10, and even 14 ML (see Ref. 34). The divergence can come from different techniques employed in the growth of these thin films. However none of the works had focus special attention in defects such as stacking faults during deposition at the interval of 10 and 14 deposited ML, where dislocations occurred only in some (111) planes. The three different approaches for the analysis of the growth process used in the present study showed excellent agreement.

IV. CONCLUSIONS

The present work studied the deposition of Pd thin films on Au(100). By growing the thin film layer by layer with MD simulations, we showed that films with less than 10 ML grew in the fcc structure under stress as both of the analysis of the angular function distribution as recently reported by Ackland and Jones and the centrosymmetry parameter indicated. After 10 ML, the stress relaxed in the Pd film, forming defects in the structure, identified as stacking faults with hcp structure. The change in the fcc symmetry structure measured by centrosymmetry parameter (c), where we obtained $0.04 < c < 0.08$ for the atoms forming the defects, in good agreement with stacking faults in the fcc structures. To get a quantitative evaluation of this process the calculated stress tensor evolution showed a change in increment of stress-thickness product, changing from $(\Delta\sigma \cdot h)/\mathrm{ML} = 2.83$ GPa Å/ML to $(\Delta\sigma \cdot h)/\mathrm{ML} = 1.5$ GPa Å/ML when the formation of defects started in the film. Therefore, by the use of these three independent methods of analysis of the growth process we could give a consistent and interesting account of the understanding of the effects that occur in this process. By this perspective, our work contributes to understanding of the growth of Pd on Au(001) and we reported new directions for analysis of structures and defects in Pd on Au(001). We hope that our results could be of interest to experimentalists growing metal thin films.

ACKNOWLEDGMENTS

We Thank Rickson Mesquita for a critical reading of the manuscript. Simulations were performed at the Centro Nacional de Computacao de Alto Desempenho (CENAPAD-SP) and at the Institute of Physics "Gleb Wataghin" (IFGW) both in Sao Paulo. This work was supported by Fundacao de Amparo a Pesquisa do Estado de Sao Paulo (FAPESP), Conselho Nacional de Desenvolvimento Cientifico e Tecnologico (CNPq), and CAPES. Z.S.P. thanks CNPq and CAPES for research grants.

[1] B. M. Ocko, I. K. Robinson, M. Weinert, R. J. Randler, and D. M. Kolb, Phys. Rev. Lett. **83**, 780 (1999).
[2] M. A. Pfeifer, O. Robacha, B. M. Ockob, and I. K. Robinson, Physica B **357**, 152 (2005).
[3] Z. S. Pereira and E. Z. da Silva, Phys. Rev. B **79**, 115404 (2009).
[4] Y. Nishihata, J. Mizuki, T. Akao, H. Tanaka, M. Uenishi, M. Kimura, T. Okamoto, and N. Hamada, Nature (London) **418**, 164 (2002).
[5] B. Sampedro, P. Crespo, A. Hernando, R. Litran, J. C. Sanchez Lopez, C. Lopez Cartes, A. Fernandez, J. Ramirez, J. Gonzalez Calbet, and M. Vallet, Phys. Rev. Lett. **91**, 237203 (2003).
[6] R. Litrán, B. Sampedro, T. C. Rojas, M. Multigner, J. C. Sanchez-Lopez, P. Crespo, C. Lopez-Cartes, M. A. Garcia, A. Hernando, and A. Fernandez, Phys. Rev. B **73**, 054404 (2006).
[7] T. Shinohara, T. Sato, and T. Taniyama, Phys. Rev. Lett. **91**, 197201 (2003).
[8] Y. Oba, H. Okamoto, T. Sato, T. Shinohara, J. Suzuki, T. Nakamura, T. Muro, and H. Osawa, J. Phys. D **41**, 134024 (2008).
[9] Y. Oba, T. Sato, and T. Shinohara, Phys. Rev. B **78**, 224417 (2008).
[10] S. S. Alexandre, E. Anglada, J. M. Soler, and F. Yndurain, Phys. Rev. B **74**, 054405 (2006).
[11] V. L. Moruzzi and P. M. Marcus, Phys. Rev. B **39**, 471 (1989).
[12] F. Aguilera-Granja, J. M. Montejano-Carrizalesa, and A. Vega, Solid State Commun. **133**, 573 (2005).
[13] J. de la Figuera, F. Leonard, N. C. Bartelt, R. Stumpf, and K. F. McCarty, Phys. Rev. Lett. **100**, 186102 (2008).
[14] W. Obretenov, U. Schmidt Muller, W. J. Lorenz, G. Staikov, E. Budevski, D. Carnal, U. Müller, H. Siegenthaler, and E. Schmidt, J. Electrochem. Soc. **140**, 692 (1993).
[15] A. M. Bittner, J. Wintterlin, and G. Ertl, Surf. Sci. **376**, 267 (1997).
[16] T. O. Menteş, A. Locatelli, L. Aballe, and E. Bauer, Phys. Rev. Lett. **101**, 085701 (2008).
[17] C. Liu and S. D. Bader, Phys. Rev. B **44**, 12062 (1991).
[18] B. Shan, L. Wang, S. Yang, J. Hyun, N. Kapur, Y. Zhao, J. B. Nicholas, and K. Cho, Phys. Rev. B **80**, 035404 (2009).
[19] X. W. Zhou, R. A. Johnson, and H. N. G. Wadley, Phys. Rev. B **69**, 144113 (2004).
[20] S. M. Foiles, M. I. Baskes, and M. S. Daw, Phys. Rev. B **33**, 7983 (1986).
[21] S. J. Plimpton, J. Comput. Phys. **117**, 1 (1995).
[22] H. Van Swygenhoven, P. M. Derlet, and A. G. Froseth, Nature Mater. **3**, 399 (2004).
[23] I. L. Dillamore, R. E. Smallman, and W. T. Roberts, Philos. Mag. **9**, 517 (1964).
[24] W. G. Hoover, Phys. Rev. A **31**, 1695 (1985).
[25] G. J. Ackland and A. P. Jones, Phys. Rev. B **73**, 054104 (2006).
[26] L. D. Landau and E. M. Lifshitz, *Theory of Elasticity* (Pergamon, New York, 1970).
[27] C. L. Kelchner, S. J. Plimpton, and J. C. Hamilton, Phys. Rev. B **58**, 11085 (1998).
[28] J. Li, in *Handbook of Materials Modeling*, edited by S. Yip (Springer, New York, 2005), p. 1051.
[29] T. Zhu, J. Li, A. Samanta, H. G. Kim, and S. Suresh, Proc. Natl. Acad. Sci. U.S.A. **104**, 3031 (2007).
[30] C.-W. Pao, S. M. Foiles, E. B. Webb, D. J. Srolovitz, and J. A. Floro, Phys. Rev. Lett. **99**, 036102 (2007).

[31] C.-W. Pao and D. J. Srolovitz, Phys. Rev. Lett. **96**, 186103 (2006).
[32] C.-W. Pao and D. J. Srolovitz, J. Mech. Phys. Solids **54**, 2527 (2006).
[33] A. K. Subramaniyan and C. T. Sun, Int. J. Solids Struct. **45**, 4340 (2008).
[34] A. L. N. Pinheiro, M. S. Zei, M. F. Luo, and G. Ertl, Surf. Sci. **600**, 641 (2006).